Talanta Open 5 (2022) 100114

Contents lists available at ScienceDirect

Talanta Open

journal homepage: www.sciencedirect.com/journal/talanta-open

Detection of N-phenylpropanamide vapor from fentanyl materials by secondary electrospray ionization-ion mobility spectrometry (SESI-IMS)

Charles D. Smith [a], Ashley C. Fulton [b,*], Mark Romanczyk [c], Braden C. Giordano [c], Christopher J. Katilie [d], Lauryn E. DeGreeff [e]

[a] National Research Council Post-Doctoral Fellow, U.S. Naval Research Laboratory, 4555 Overlook Ave SW, Washington, DC 20375, USA
[b] American Society for Engineering Education Post-Doctoral Fellow at Naval Research Laboratory, 4555 Overlook Ave. SW, Washington, DC, USA
[c] Naval Research Laboratory, Chemistry Division, Code 6181, 4555 Overlook Ave. SW, Washington, DC, USA
[d] Nova Research Inc., 1900 Elkins St., Alexandria, VA, USA
[e] Formerly Naval Research Laboratory, Chemistry Division, Code 6181, 4555 Overlook Ave. SW, Washington, DC, USA

ARTICLE INFO

Keywords:
Opioid
Fentanyl
N-phenylpropanamide (NPPA)
Headspace
Ion mobility spectrometry
Secondary electrospray ionization
Vapor phase

ABSTRACT

Opioids pose a serious health risk to abusers and law enforcement officials responsible for detecting and handling these classes of drugs. Given the dangers posed by this class of drugs, fentanyl in particular, non-contact detection methods are highly desired. Determination of fentanyl vapor signature enables the identification of target analytes for the indirect detection of the parent opioid without direct sample handling. Diluted N-phenylpropanamide (NPPA), a degradant of fentanyl, was injected into a bench-top ion mobility spectrometer (IMS) to develop a method to detect NPPA in solution. The same parameters were used to assist in developing a method for gas phase NPPA detection. By varying the source voltage and direct spray and mass flow rates, the effects of system impurities were minimized. Weak and strong acids were then added to the electrospray solvent and gas phase NPPA was detected from the headspace of masses of 5 mg or greater of pure fentanyl.

1. Introduction

Fentanyl was developed in the 1960s for pain-relief purposes with overdoses first reported in the 1980s [1–3]. This opioid known to be 50–100 times stronger than morphine has become more well-known in recent years for illicit use. In 2019, overdose deaths due to synthetic opioids totaled 36,359, an increase of 1040% from 2013, mainly attributed to fentanyl [4]. Fentanyl is often found mixed with other drugs abused, and overdose reports noted that users were unaware of the presence of fentanyl [5]. The lack of awareness raises serious safety concerns for not only users but individuals responsible for its detection and handling in the field. Those responsible for detection should avoid direct interaction, especially with a fentanyl, as it only requires milligrams to be considered lethal [6].

The low vapor pressure of fentanyl, $5.9 \pm 4.7 \times 10^{-7}$ Pa [7], makes direct detection in the gas phase arduous. Therefore, the vapor signature of fentanyl is required to indirectly detect the parent opioid in the vapor phase. For those compounds with low vapor pressures, the associated headspace may be accompanied by the solvents used in synthesis, degradation products, or manufacturing impurities. Lurie et al. noted the presence of 40 different processing impurities in fentanyl synthesis, particularly those associated with the Janssen or Siegfried syntheses, using UHPLC-MS-MS [8]. Vaughan et al. (2021a) used SPME-GC–MS to study undiluted pharmaceutical grade fentanyl in order to provide a vapor signature. Two of the three most abundant compounds, *N*-phenethyl-4-piperidone (NPP) and *N*-phenylpropanamide (NPPA) were positively identified and also unaffected when adulterated with lactose, mannitol, or initosol [9]. In agreement, Vaughan et al. (2021b) also detected NPPA from the headspace of confiscated fentanyl materials [10]. NPP is a known precursor in fentanyl synthesis and categorized as List I Chemical by the DEA, a designation used for compounds used in manufacturing of illicit drugs, limiting the amount that can be ordered. No such restriction exists for NPPA, a fentanyl manufacturing impurity, and gram quantities are available for purchase.

Multiple detection techniques are available for first responders of a suspected drug overdose, clandestine laboratory, or other crime scene. Colorimetric techniques are available for multiple families of illicit drugs [11–13] with results based on the color(s) observed after sample reaction with specific reagents. Results are generated quickly, require minimal operator training, but sample contact is necessary, putting

* Corresponding author.
E-mail address: ashley.fulton.ctr@nrl.navy.mil (A.C. Fulton).

https://doi.org/10.1016/j.talo.2022.100114
Received 29 December 2021; Received in revised form 28 March 2022; Accepted 30 March 2022
Available online 10 April 2022

medical or law enforcement personnel at risk. Mass spectrometric (MS) techniques offer picogram limits of detection [14,15], though, while sensitive, these instruments are expensive and require extensive operator training [16]. Ion mobility spectrometry (IMS) offers an affordable alternative to MS without the need of skilled operators as built-in instrument libraries are available. Sisco et al. applied fentanyl and 16 fentanyl analogues to meta-aramid wipes, which were inserted into the IMS. While nanogram level sensitivity was reported, sample contact was still necessary [17]. IMS devices capable of vapor phase detection are available, preventing operator contact, but a method for fentanyl detection has yet to be developed.

In IMS, sample ions are transported from source to detector in a drift tube by using an applied electric field against a flow of drift gas, usually air or nitrogen. Peak intensities are plotted as a function of analyte ion drift time, which is dependent on drift tube length, temperature, pressure, and potential as well as ion collisional cross section [18,19]. Ionization of the target analyte is essential to allow for detection. One method of ionization is electrospray ionization (ESI). In ESI, ionization begins with a fine mist of diluted sample generated by an electrospray needle held at a fixed potential. The droplets emit an excess of positive or negative charge depending on the potential. The quantity of charge in solution can also be enhanced through the addition of a weak acid or base. Solvent molecules are rapidly evaporated in the heated sample chamber until the droplets approach the Rayleigh limit, leading to even smaller, charged droplets with radii in the nanometer range [20]. For example, Midey et al. ionized methamphetamine, cocaine, and morphine using 0.5% (%v/v) acetic acid in 90:10 methanol:water with an electrospray ionization source [21] with the same IMS used herein. Under these conditions, sample preparation and, therefore, contact would still be required.

Commercial handheld IMS devices are capable of vapor detection, which would advantageously prevent the operator from directly contacting the sample. Before employing such devices for fentanyl detection, the compounds in the headspace must be detected on a benchtop IMS. Mullen et al. introduced trinitrotoluene (TNT) and 2,6-dinitrotoluene (2,6-DNT) vapor to the sample chamber of the IMS, separately from the methanol electrospray solvent [22]. This method of introducing sample and electrospray solvent is known as secondary electrospray ionization (SESI) [23]. In the method described herein, NPPA will be introduced to the sample chamber perpendicular (Fig. 1) to the reactant ions introduced by the electrospray source.

This work will describe the development of a semi-quantitative method using SESI-IMS to enable the identification of NPPA in the vapor phase without manipulation of the substance. NPPA was ionized using a commercially available bench top IMS in solution and pure vapor phase, and from fentanyl headspace via SESI and subsequently detected on a Faraday plate detector. This research will facilitate the field detection of NPPA vapor as an indicator for the presence of fentanyl. Development of a field-deployed non-contact detection method will allow for first responders to identify fentanyl at a scene without risk of exposure due to contact with the substance.

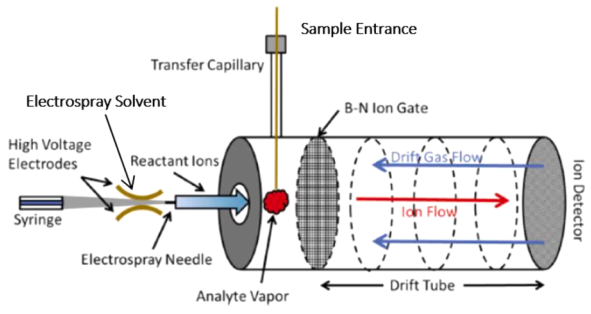

Fig. 1. Side view diagram of the IMS used [22]. Reprinted with permission of Elsevier.

2. Materials and methods

2.1. Chemicals

NPPA was purchased from Toronto Research Chemicals (Toronto, Ontario, Canada) and used as received. ACS grade methanol, acetic acid, formic acid, and hydrochloric acid were purchased from Fisher Scientific (Waltham, MA). 18 MΩ Milli-Q H_2O was used. Tryptophan was purchased from Sigma-Aldrich (St. Louis, MO). Pharmaceutical-grade fentanyl was purchased from Cayman Chemicals (Ann Arbor, MI, USA).

2.2. Instrumentation

Ion mobility spectra were collected by using a GA2100 Ion Mobility Spectrometer (Excellims, Acton, MA) with an Excellims-designed Directspray™ ionization source with a 100 μL gas tight syringe (Hamilton, Reno, NV) attached to an electrospray needle. Instrument layout is discussed elsewhere [21]. Briefly, the electrospray solvent or sample solution were introduced to the ionization chamber using the parameters listed in Table 1. The electrospray needle was 33 gage stainless steel with an inner diameter of approximately 110 μm. An Excellims guard was attached to the end of the syringe to protect the needle. The instrument was calibrated with a 0.1 mg/mL tryptophan solution in an 80:20 mixture of methanol to water according to manufacturer recommendations. The IMS was equipped with VisIon software for data acquisition and analysis. The individual spectra displayed are an average of 25 spectra collected over 35 s. Slight differences in drift time during data collection may cause non-Gaussian characteristics in the resulting peaks. Intensities, or volts, were plotted as a function of analyte drift time.

Ion Source Collision-Activated Dissociation (IS-CAD) was performed by using a Thermo Scientific LTQ mass spectrometer (Thermo Scientific, San Jose, CA, USA) equipped with an Electrospray Ionization source. NPPA was diluted in methanol at a concentration of 5 ppm and directly injected into the probe at flow rate of 2.0 μL min^{-1}. The ionization conditions were as follows: ESI spray voltage 3.5 kV, capillary temperature 250 °C and capillary voltage 50 V. The tube lens was changed by increments of 10 V to facilitate IS-CAD measurements. Nitrogen gas was employed as sheath and auxiliary gas at 8 and 3 arbitrary units, respectively.

2.3. Methods

For gas phase detection, solid NPPA and fentanyl were put into 22 mL PFA vials purchased from Savillex (Eden Prairie, MN) and inserted into the Mixed Vapor Generation device (MV-Gen) for vapor generation, as described [24]. Briefly, the MV-Gen is an air tight, two-compartment device used for vapor delivery. When latched together, the two compartments are encased within a water jacket allowing for temperature control. The device has four vial slots, three of which were filled with capped, empty vials to minimize vapor dilution. The MV-Gen was

Table 1
Default IMS instrument parameters.

Default Instrument Parameters	
Source Voltage	2500 V
Drift Tube Voltage	7500 V
Source Temperature	180 °C
Drift Tube Temperature	180 °C
Direct Spray Flow Rate	2.0 μL•min^{-1}
Drift Gas Flow Rate	1.65 L•min^{-1}
Exhaust Pump Flow Rate	1.44 L•min^{-1}
Gate Voltage	90 V
Gate Pulse Width	160 μs
Drift Tube Length	10.5 cm
Polarity	+

connected to the IMS with a Teflon tube, soaked in methanol when not in use. This connection port was capped when NPPA was measured in solution. Air enters at the base of the MV-Gen and exits at the top, allowing for sample vapor transport from the source to the instrument. Samples were allowed to equilibrate in the MV-Gen overnight (*i.e.*16 h) under ambient conditions. Water was then circulated from the lower to upper water jackets of the MV-Gen with a Thermo Scientific (Waltham, MA) PC 200 Immersion Circulator at a temperature of 25 °C for one hour. Vapors were transported from the MV-Gen to the IMS using an MKS (Andover, MD) M100B Mass Flo device with an MKS Multi-Gas Controller 647C at a flow rate of 10.0 mL/min. This was the maximum allowable flow rate for this device. A SmartTrak® 2 Series 100 Mass Flow Controller (Sierra Instruments, Monterrey, CA) was used for higher mass flow rates.

The electrospray solvent was drawn into the gas-tight syringe for introduction into the sample chamber. For SESI, all solutions were made at respective concentrations in 80:20 methanol to water. Reactant ions were generated through the application of a high potential to the electrospray needle allowing for ionization of the analyte vapor introduced via the transfer capillary from the MV-Gen (Fig. 1). Sample ions were introduced into the drift tube through a Bradbury-Nielson gate and detected with a Faraday plate detector against the air drift gas provided by an Environics (Tolland, CT) Model 7000 Zero Air generator. Air flow to the mass flow controller was also provided by this device.

Reduced ion mobilities ($K_{O,sample}$) were calculated using sample drift

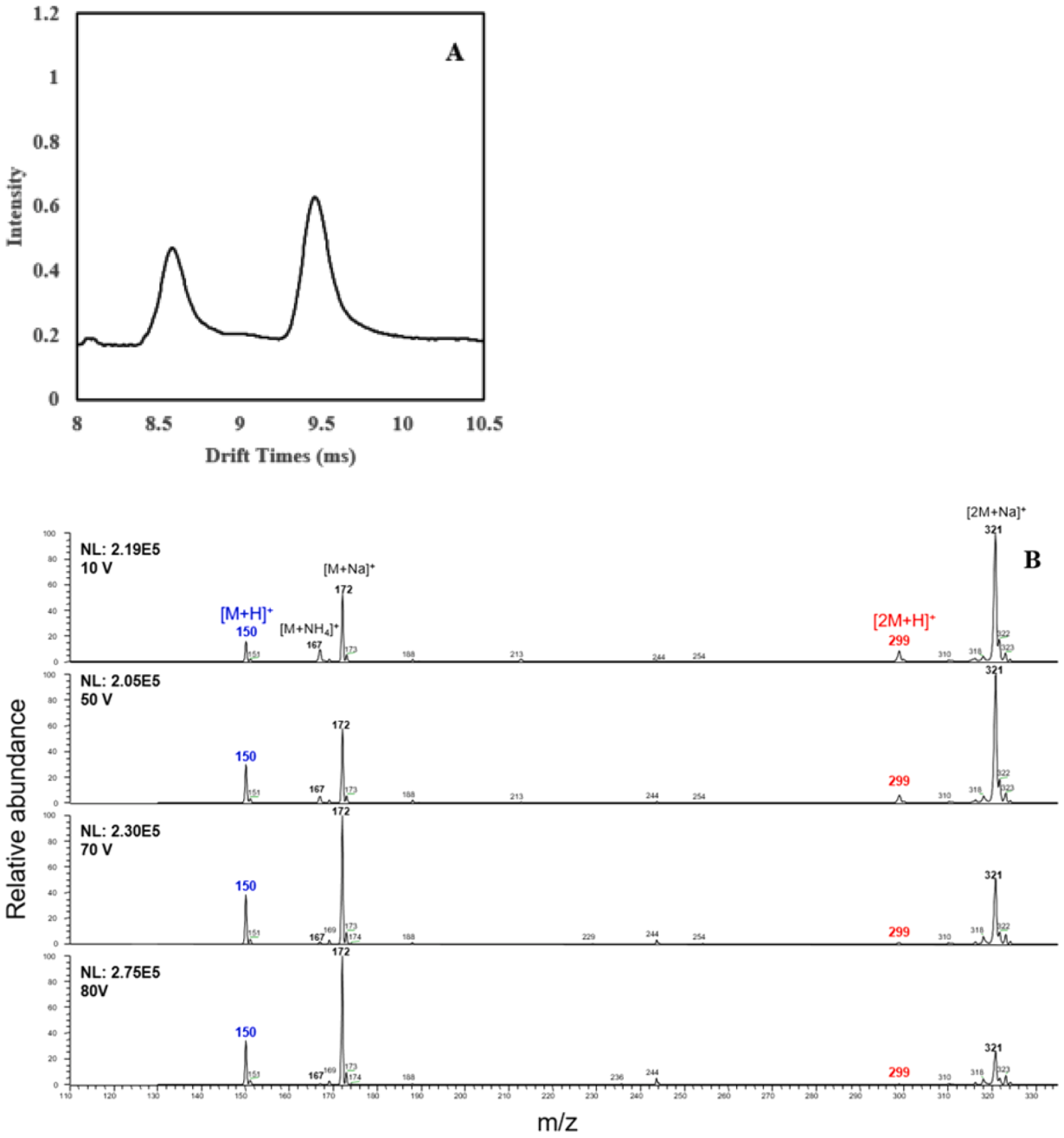

Fig. 2. A, B**:** Mobility spectrum of 5 ppm NPPA in methanol with Table 1 parameters (A). (+) Electrospray ionization MS^1 spectra of ionized NPPA diluted in methanol at a concentration of 5 ppm at different tube lens voltages. Ions of *m/z* 150 and 299 corresponded to protonated NPPA and the proton-bound dimer of NPPA, respectively. Ions of *m/z* 172 and 321 are sodium adducts of ions of *m/z* 150 and 299, respectively. Ions of *m/z* 167 are ammonium adducts of NPPA. As the tube lens voltage increased, the abundances of *m/z* 150 increased and *m/z* 299 decreased. The sodium adducts of *m/z* 172 and 321 showed the same trend supporting that there detection were depended on the presence of ions of *m/z* 150 and 299, respectively (B).

time ($t_{d,sample}$) by using Eq. (1) [18] and an accepted tryptophan reduced ion mobility ($K_{0,standard}$) of 1.39 cm^2/V•s [25] with a drift time ($t_{d,standard}$) of 10.21 ms programmed into the instrument.

$$\frac{K_{0,\ sample}}{K_{0,\ standard}} = \frac{t_{d,standard}}{t_{d,sample}} \quad (1)$$

3. Results and discussion

3.1. NPPA peak identification measurements

A 5 ppm NPPA in methanol solution was first injected into the IMS using the default instrument parameters (Table 1) to note the location of any NPPA peak(s). As shown by Fig. 2, NPPA exhibits two peaks at approximately 8.7 ms and 9.5 ms, likely a monomer and dimer, respectively [26]. Using Eq. (1) the calculated reduced ion mobilities were 1.47 ± 0.03 and 1.62 ± 0.03 cm^2/V•s.

To confirm the presence of the dimer at 9.5 ms, the same solution was directly injected into a Thermo LTQ ion trap mass spectrometer by using an Electrospray Ionization (ESI) probe operated in the positive ion mode. Protonated ions of NPPA were detected corresponding to ions of *m/z* 150 as well as ions of *m/z* 299 (Fig. S1). Efforts to subject ions of *m/z* 299 to tandem mass spectrometry were attempted, but during ion isolation, the signal of the ions were not detected. Consequently, MS^2 product ion spectrum for ions of *m/z* 299 were not collected. However, in-source collision-activated dissociation (IS-CAD) was completed by increasing the tube lens voltage. This activation method does not involve an isolation step prior to activation and is successful at providing structural information [27]. For IS-CAD, as the tube lens voltage increases, the internal energy deposited into ions through collisions with the residual background gasses increases. Hence, if ions of *m/z* 299 were dimers of NPPA, the ratio of the abundances of ions of *m/z* 150 to *m/z* 299 would likely increase as a function of increasing the tube lens voltage. For IS-CAD measurements, the tube lens voltage was increased by increments of 10 V and the abundances of ions of *m/z* 150 and 299 were recorded. As the tube lens voltage increased, the ratio of ions of

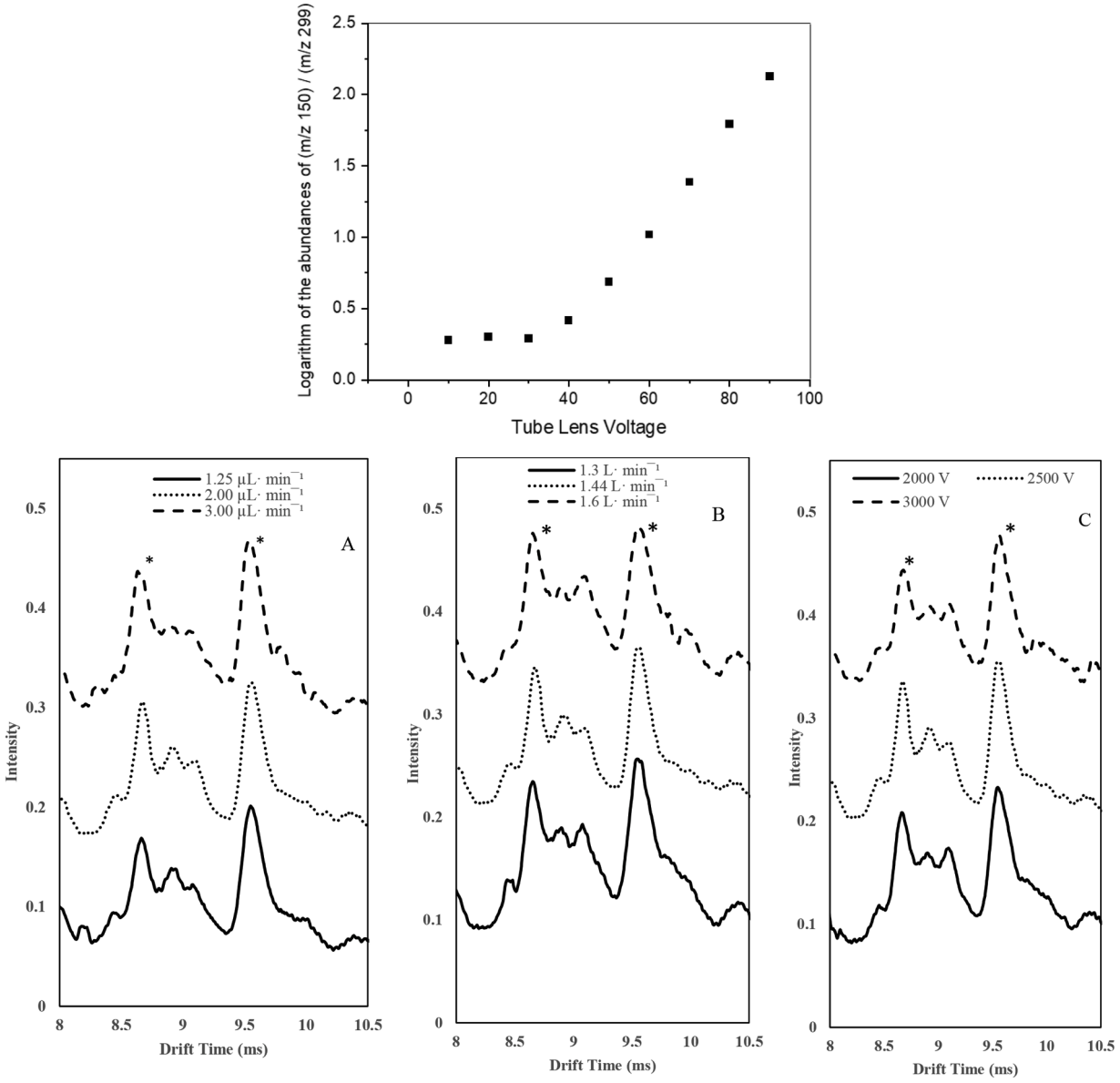

Fig. 3. The plot of the logarithm of the abundances of (*m/z* 150) / (*m/z* 299) as a function of tube lens voltage. As the voltage increased, the abundances of ions of *m/z* 150 increased and *m/z* 299 decreased supporting that ions of *m/z* 299 were likely derived from the protonated monomers of NPPA (*m/z* 150). Fig. 3A–C: Effect of direct spray flow rate (A), exhaust pump flow rate (B), and source voltage (C) on NPPA (*) signal in a 250 ppb solution. Methanol was used as the solvent and the Table 1 parameters applied. The intensities have been shifted for a clearer comparison.

m/z 150 to 299 increased (Fig. 3 and Table S1). Hence, ions of *m/z* 299 were likely proton-bound dimers as the abundances of ions of *m/z* 150 steadily increased, but the ions of *m/z* 299 decreased as a function tube lens voltage.

3.2. Method optimization for NPPA in solution

Method parameters were varied from the default settings (Table 1) for a 250 ppb NPPA in methanol solution to optimize analyte signal. The signals observed for the two NPPA peaks observed at approximately 8.7 ms and 9.5 ms were compared to that obtained with the default parameters to assess effects. Source voltage was varied from 2000 V-3000 V to optimize the concentration of reactant ions while minimizing the risk of analyte ion degradation. Shumate et al. looked at the effect on total ion current (TIC) as a function of needle voltage using methanol. The TIC, or analyte signal, increased as a function of applied voltage [28]. Mullen et al. noted a corona discharge (CD) produced with the IMS used herein at a source voltage of 3200 V [22]. However, analyte degradation and, therefore, potential loss of signal was observed with corona discharge ionization sources [29]. Hence, the source voltage was varied from 2000 to 3000 V. Fig. 3C shows the effects of source voltage on NPPA signal. A maximum is observed at 2500 V and it did not appear that the larger source voltage produced additional reactant ions. The direct spray flow rate was also varied from 1.25 to 3.0 μL·min^{-1}. Shumate et al. also noted a decreased TIC with increased flow rate [28]. Nonetheless, an increased flow rate will introduce more sample to the ionization chamber, and potentially additional ions, if efficient sample ionization occurs. The peak signals observed for the direct spray flow rate (Fig. 3A) do increase from 1.25 μL·min^{-1} to 2.0 μL·min^{-1} but not from 2.0 μL·min^{-1} to 3.0 μL/min^{-1}. For practicality and to minimize solvent waste, 2.0 μL·min^{-1} was used for further experiments with NPPA in solution. The exhaust pump is used to cool the electrospray needle and push non-solvated droplets out of the ionization chamber. As shown by Fig. 3B, the intensities for the two NPPA peaks are between 0.1–0.15 and seem relatively unaffected by this parameter. This parameter was also kept at the default setting. Based on the data observed in Fig. 3A–C, the default parameters would be used in the initial NPPA vapor phase experiments.

3.2. Method optimization for NPPA in the vapor phase

Vapor phase NPPA detection by IMS required further method development due to the introduction of the mass flow controller, the device responsible for transporting sample vapor from the MV-Gen to the IMS.Beginning experiments were done with air blanks (Fig. 4A) to ensure system impurities, if any, would not interfere with NPPA detection. System impurities were observed with flow rates ≥ 30 mL·min^{-1}. The MKS Mass Flow Device was set to 10 mL·min^{-1} for vapor introduction into the IMS.

An NPPA sample mass of 856 mg was initially used to ensure an ample supply of vapor phase analyte. By applying the default instrument parameters (Table 1) discussed above and using methanol as the solvent to generate the electrospray, NPPA was not detected. Given the volatility of NPPA [9], it was suspected that issues associated with detection under these initial conditions were related to ionization efficiency, and acids of varying strength were then added to the secondary electrospray solvent.

3.3. Optimization of secondary electrospray solvent

Weak organic acid addition to the electrospray solvent is common practice [21,23,30]. In positive-ion SESI, weak acids, such as formic and acetic acids, protonate analytes with neutral or basic functionalities. NPPA is a secondary amide with an approximate pKa value of 16 making it a basic analyte appropriate for use with a weak acid in SESI. A 50 ppm acetic acid solution was added to the electrospray inlet. The flow rate of 1.0 μL/min. was chosen to decrease system impurities observed with the

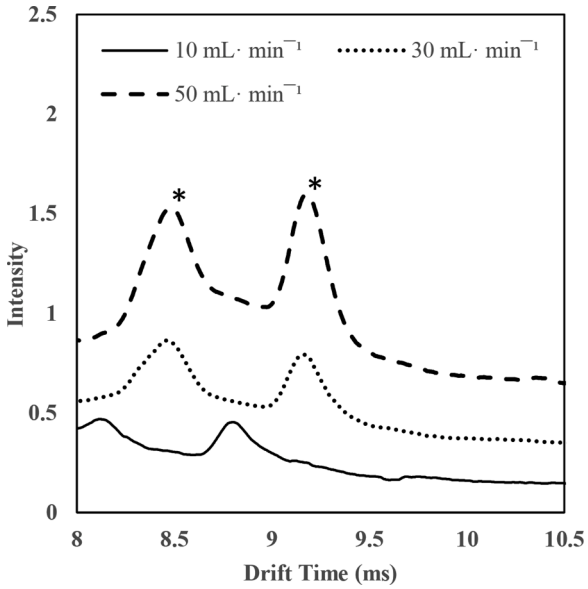

Fig. 4. Effect of mass flow rate on instrument baseline with air samples. Baseline contaminants (*) are labeled. Table 1 parameters were used with the exception of a 3500 V source voltage and the SmartTrak® 2 Series 100 Mass Flow Controller.

acetic acid solution at flow rates ≥1.5 μL/min. As shown by Fig. 5, a blank mobility spectrum of the acetic acid electrospray solvent exhibits a flat baseline in the area of interest, free of system impurities. When gas phase NPPA was introduced to the IMS, two NPPA peaks were observed in agreement with that observed in solution. The second of the two NPPA peaks observed in Fig. 5 almost overlap with $K_0 = 1.43 \pm 0.01$ and 1.47 ± 0.03 cm^2/V•s (Fig. 5A) for NPPA vapor and in solution, respectively.

The first peak observed for NPPA vapor and in solution exhibited K_0 values of 1.54 ± 0.01 cm^2/V•s and 1.61 ± 0.01 cm^2/V•s, respectively. The monomer ion peak shift observed in Fig. 5A is not due to acetic acid adducts as they are not detected in Fig. 5B. The $[M + H]^+$ and $[M + Na]^+$ monomer ions are detected in both Figs. 2B and 5B, meaning the monomer ion peak observed is not due to the preferred ionization of one ionic species over the other. The reason for the observed sodium adducts remains unknown but there are literature reports of $[M + Na]^+$ even when Na^+ was not in solution [33]. The blank mobility spectrum in Fig. 5A is also relatively flat in the area of interest so the artifact peaks due to acetic acid in Fig. 5B (*i.e. m/z* 165 and 340) are not interfering in the collection of the NPPA vapor mobility spectrum. The variability in K_0 values is well-documented in IMS literature. Caffeine, for example, has published K_0 values ranging from 1.52 to 1.59 cm^2/V•s [31,32]. Therefore, the K_0 values were still considered in agreement for the first of the two NPPA peaks.

A comparison of NPPA peak intensities for Figs. 3A–C, and 5 show the improved sensitivity provided by the addition of acetic acid to the secondary electrospray solvent. With the Table 1 parameters used, the exact monomer ion peak intensities for the 0.25 mg/L and 10 mg/L NPPA solutions are 0.13 and 1.75 V, respectively, an improvement of only 13.5.The sensitivity observed with gas phase NPPA and acetic acid secondary electrospray solvent was more than satisfactory given the ability to detect as little as 10 mg NPPA. Methanol only as the secondary electrospray solvent clearly weakens method sensitivity and this is further supported by the fact that 856 mg NPPA was not detected.

The expected amount of NPPA present in the headspace associated with a small fentanyl sample is expected to be significantly less than the amount associated with the 856 mg NPPA sample used in method optimization. Therefore, the amount of NPPA was decreased to 10 mg. The 10 mg sample showed a prominence of the second peak in the

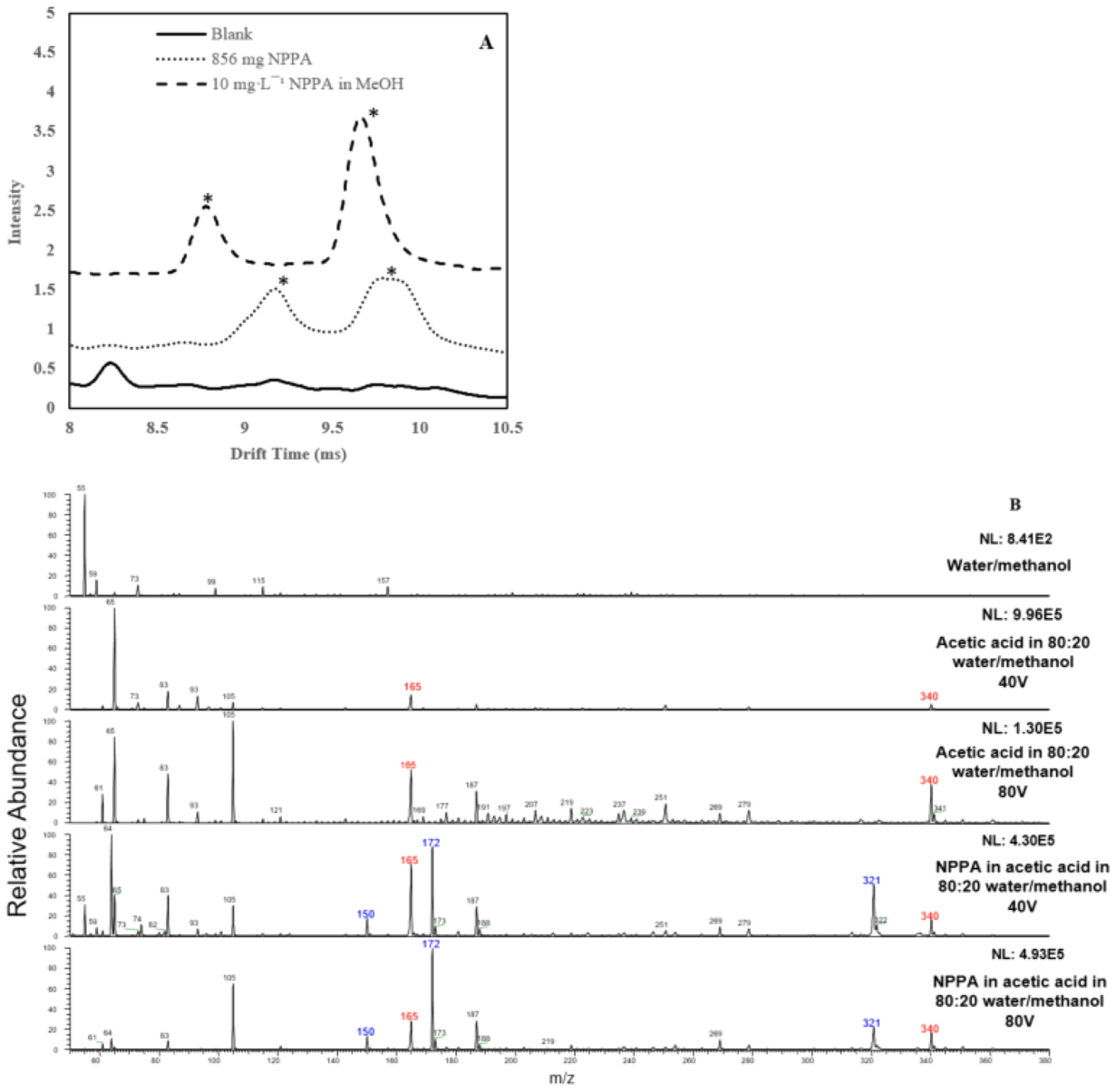

Fig. 5. A,B: (A) Mobility spectrum of blank 50 ppm acetic acid solution in syringe and used with 856 mg NPPA; 10 ppm NPPA in MeOH introduced via syringe port. (*) indicates peak associated with NPPA. The intensities have been shifted for a clearer comparison. Direct spray flow rate = 1.0 μL/min.; source voltage = 2500 V; mass flow controller flow rate = 10 mL/min. (B) Electrospray Ionization MS^1 spectra of ionized 5 ppm NPPA in 50 ppm acetic acid diluted in 80:20 methanol:water at tube lens voltages of 40 and 80 V. Ions of *m/z* 150 correspond to protonated NPPA monomer. Ions of *m/z* 172 and 321 are sodium adducts of the NPPA monomer and dimer ions, respectively. Trends observed in Fig. 2B with respect to lens voltages are also observed. The ions *m/z* 165 and 340 are present in background upon the addition of acetic acid. Blank mobility spectra are presented for 80:20 methanol/water, 50 ppm acetic acid in 80:20 water/methanol at a lens voltage of 40 V, and 50 ppm acetic acid in 80:20 water/methanol at a lens voltage of 80 V. Normalization levels (NL) are indicated.

doublet observed in previous experiments with K_0 = 1.47 $cm^2/V•s$ (Fig. 6). Holness et al. reported that an increased acid concentration will increase analyte ionization ability, especially important for mixtures with a wide range of proton affinities [34]. Formic acid was tested as a means of protonation and since it is slightly stronger than acetic acid, it was hypothesized to give a highly resolved signal for NPPA. Unfortunately, the 50 ppm formic acid solution resulted in a decreased peak intensity and shifted all peaks, making it difficult to compare with previous data as shown in Fig. 6. A dilute solution of a strong acid could also bridge the gap of ionization capability and peak intensity. To test this theory, a 0.5 ppm HCl solution was used which resulted in an increase in peak intensity for 10 mg. In contrast to that observed with the weaker acids (Fig. 5), NPPA exhibited a single peak when ionized with a dilute HCl electrospray. Given the acid strength of HCl relative to acetic acid, additional NPPA should be protonated, increasing the dimer concentration observed, resulting in an increased dimer ion peak intensity. An increased HCl concentration should increase the signal of the first NPPA peak as well. However, an increased concentration of HCl risks damage to the IMS and, therefore, was not used. Nonetheless, a higher resolving power was achieved using the HCl solution which will allow for the optimal identification of fentanyl using NPPA.

The sample size of NPPA was further decreased to 5 mg, and, additionally, vapor from 5 mg of fentanyl was also tested. The vapor from a 5 mg sample of NPPA gave an evident peak at K_0 = 1.46 $cm^2/V•s$. When testing the vapor from a 5 mg sample of fentanyl a comparable peak at K_0 = 1.47 $cm^2/V•s$ was also shown as seen in Fig. 7. A direct liquid injection of fentanyl confirmed the NPPA observed in vapor analysis was from the headspace of fentanyl and not the substance (Fig. 7).

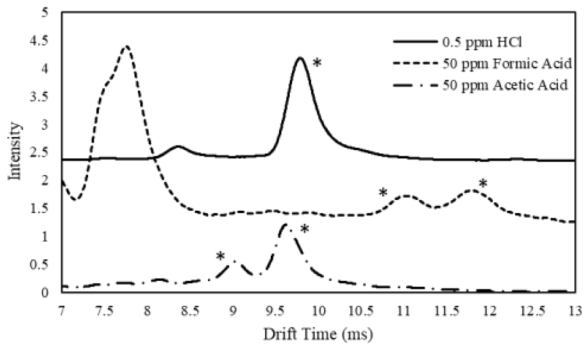

Fig. 6. Effects of weak acids on the vapor from 10 mg sample of NPPA. (*) indicates peak associated with NPPA. The intensities have been shifted for a clearer comparison. Table 1 parameters used.

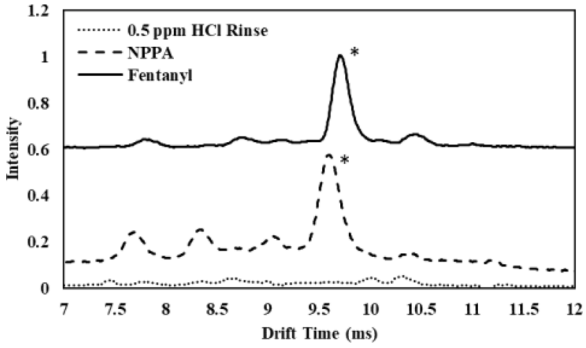

Fig. 7. Comparison of vapor from a 5 mg sample of NPPA and the vapor from a 5 mg sample of fentanyl using a 0.5 ppm HCl solution in SESI. (*) indicates peak associated with NPPA. The intensities have been shifted for a clearer comparison. Table 1 parameters used.

4. Conclusion

In the work discussed, vapor phase NPPA was detected allowing for indirect identification of fentanyl. Methods for solution and gas phase detection of NPPA were developed and optimized. Particular care was taken to minimize the effects of system impurities on the instrument baseline. When these impurities were addressed, modification of the electrospray solvent with hydrochloric acid greatly improved detection. Vapor phase NPPA was detected above 5 mg of NPPA, as well as from the headspace of solid fentanyl. The work discussed herein will allow for eventual non-contact fentanyl detection with a handheld IMS.

Funding

This project was supported through an Interagency Agreement with the National Institute of Justice, Office of Justice Programs, U. S. Department of Justice, The opinions, finding and conclusions, or recommendations expressed are those of the author(s), and do not necessarily reflect those of the U.S, Department of Justice or any of its components. This research was performed while the authors held an NRC and ASEE Research Associateship awards at the Naval Research Laboratory.

Declaration of Competing Interest

The authors declare that they have no known competing financial interests or personal relationships that could have appeared to influence the work reported in this paper.

Acknowledgements

The authors would like to acknowledge Julia Kaszycki and Eugenie Hainsworth of the Excellims Corporation. Their expertise on instrument operation and maintenance has been invaluable.

References

[1] P. Armenian, K. Vo, J. Barr-Walker, K. Lynch, Fentanyl, fentanyl analogs and novel synthetic opioids: A comprehensive review, Neuropharmacology (2018) 121–132, https://doi.org/10.1016/j.neuropharm.2017.10.016.
[2] J. Garriott, R. Rodriguez, V. Di Maio, A death from fentanyl overdose, J. Anal. Toxic. 8 (1984) 288–289, https://doi.org/10.1093/jat/8.6.288.
[3] H. Silsby, D. Kruzich, M. Hawkins, Fentanyl citrate abuse among health care professionals, Mil. Med. 149 (1984) 227–228, https://doi.org/10.1093/milmed/149.4.227.
[4] C. Mattson, L. Tanz, K. Quinn, M. Kariisa, P. Patel, N. Davis, Trends and geographic patterns in drug and synthetic opioid overdose deaths-United States, 2013-2019, Morb. Mortal. Wkly. Rep. Cent. Dis. Control Prev. 70 (2021) 202–207.
[5] D. Dowell, E. Arias, K. Kochanek, R. Anderson, G. Guy, J. Losby, G. Baldwin, Contribution of Opioid-Involved Poisoning to the Change in Life Expectancy in the United States, 2000-2015, JAMA 318 (2017) 1065–1067, https://doi.org/10.1001/jama.2017.9308.
[6] Drug Enforcement Administration, 2017 National Drug Threat Assessment, DEA-DCT-DIR-040-17, U.S. Department of Justice-Drug Enforcement Administration, Washington, D.C, 2017.
[7] P. Gupta, K. Ganesan, P. Gutch, L. Manral, D. Dubey, Vapor pressure and enthalpy of vaporization of fentanyl, J. Chem. Eng. Data 53 (2008) 841–845, https://doi.org/10.1021/je7005067.
[8] I. Lurie, A. Berrier, J. Casale, R. Iio, J. Bozenko, Profiling of illicit fentanyl using UHPLC–MS/MS, Forensic Sci. Int. 220 (2012) 191–196, https://doi.org/10.1016/j.forsciint.2012.02.024.
[9] S. Vaughan, L. Degreeff, L. Forte, H. Holness, K. Furton, Identification of volatile components in the headspace of pharmaceutical-grade fentanyl, Forensic Chem. 24 (2021), 100331, https://doi.org/10.1016/j.forc.2021.100331.
[10] S. Vaughan, A. Fulton, L. DeGreeff, Comparative analysis of vapor profiles of fentalogs and illicit fentanyl, Anal. Bioanal. Chem. 413 (2021) 7055–7062, https://doi.org/10.1007/s00216-021-03670-4.
[11] R. Murray, P. Doering, L. Boothby, M. Merves, R. McCusker, C. Chronister, B. Goldberger, Putting an Ecstasy Test Kit to the Test: Harm Reduction or Harm Induction, Pharmacotherapy 23 (2003) 1238–1244, https://doi.org/10.1592/phco.23.12.1238.32704.
[12] C. O'Neal, D. Crouch, A. Fatah, Validation of Twelve Chemical Spot Tests for the detection of Drugs of Abuse, Forensic Sci. Int. 109 (2000) 189–201, https://doi.org/10.1016/S0379-0738(99)00235-2.
[13] N. Jornet-Martinez, R. Herraez-Hernandez, P. Campins-Falco, Stabilization of formaldehyde into polydimethylsiloxane composite: application to the in situ determination of illicit drugs, Anal. Bional. Chem. 411 (2019) 2141–2148, https://doi.org/10.1007/s00216-019-01644-1.
[14] E. Sisco, T. Forbes, M. Staymates, G. Gillen, Rapid analysis of trace drugs and metabolites using a thermal desorption DART-MS configuration, Anal. Methods 8 (2016) 6494–6499, https://doi.org/10.1039/C6AY01851C.
[15] J. Abonamah, B. Eckenrode, M. Moini, On-site detection of fentanyl and its derivatives by field portable nano-liquid chromatography-electron Ionization-mass spectrometry (nLC-EI-MS), Forensic Chem. 16 (2019), 100180, https://doi.org/10.1016/j.forc.2019.100180.
[16] L. Harper, J. Powell, E. Pijl, An overview of forensic drug testing methods and their suitability for harm reduction point-of-care services, Harm Reduct J. 14 (2017) 1–13, https://doi.org/10.1186/s12954-017-0179-5.
[17] E. Sisco, J. Verkouteren, J. Staymates, J. Lawrence, Rapid detection of fentanyl, fentanyl analogues, and opioids for on-site or laboratory based drug seizure screening using thermal desorption DART-MS and ion mobility spectrometry, Forensic Chem. 4 (2017) 108–115, https://doi.org/10.1016/j.forc.2017.04.001.
[18] G. Eiceman, E. Nazarov, J. Stone, Chemical standards in ion mobility spectrometry, Anal. Chim. Acta 493 (2003) 185–194, https://doi.org/10.1016/S0003-2670(03)00762.
[19] H. Borsdorf, T. Mayer, M. Zarejousheghani, G. Eiceman, Recent developments in ion mobility spectrometry, App. Spec. Rev. 46 (2011) 472–521, https://doi.org/10.1080/05704928.2011.582658.
[20] L. Konerman, E. Ahadi, A. Rodriguez, S. Vahidi, Unraveling the mechanism of electrospray ionization, Anal. Chem. 85 (2013) 2–9, https://doi.org/10.1021/ac302789c.
[21] A. Midey, A. Patel, C. Moraff, C. Krueger, C. Wu, Improved detection of drugs of abuse using high-performance ion mobility spectrometry with electrospray ionization (ESI-HPIMS) for urine matrices, Talanta 116 (2013) 77–83, https://doi.org/10.1016/j.talanta.2013.04.074.
[22] M. Mullen, B. Giordano, Combined secondary electrospray and corona discharge ionization (SECDI) for improved detection of explosive vapors using drift tube ion mobility spectrometry, Talanta 209 (2020), 120544, https://doi.org/10.1016/j.talanta.2019.120544.
[23] C. Wu, W. Siems, H. Hill, Secondary electrospray ionization ion mobility spectrometry/mass spectrometry of illicit drugs, Anal. Chem. 72 (2000) 396–403, https://doi.org/10.1021/ac9907235.

[24] L. Degreeff, C. Katilie, M. Malito, B. Giordano, Mixed Vapor Generation Device for delivery of homemade explosives vapor plumes, Anal. Chim. Acta 1040 (2018) 41–48, https://doi.org/10.1016/j.aca.2018.07.035.
[25] P. Dwivedi, A. Schultz, H. Hill, Metabolic profiling of human blood by high-resolution ion mobility mass spectrometry (IM-MS), Int. J. Mass Spectrom. 298 (2010) 78–90, https://doi.org/10.1016/j.ijms.2010.02.007.
[26] Z. Karpas, Ion Mobility Spectrometry of Aliphatic and Aromatic Amines, Anal. Chem. 61 (1989) 684–689, https://doi.org/10.1021/ac00182a009.
[27] J.T. Davidson, Z.J. Sasiene, G.P. Jackson, Comparison of in-source collision-induced dissociation and beam-type collision-induced dissociation of emerging synthetic drugs using a high-resolution quadrupole time-of-flight mass spectrometer, Int. J. Mass Spectrom. 56 (2) (2021), https://doi.org/10.1002/jms.4679.
[28] J.C.B. Shumate, H.H. Hill Jr., Coronaspray Nebulization and Ionization of Liquid Samples for Ion Mobility Spectrometry, Anal. Chem. 61 (1989) 601–606, https://doi.org/10.1021/ac00181a021.
[29] J.R. Lloyd, S. Hess, A Corona Discharge Initiated Electrochemical Electrospray Ionization Technique, J. Am. Soc. Mass Spectrom. 20 (11) (2009) 1988–1996, https://doi.org/10.1016/j.jasms.2009.07.021.
[30] R. Fernandez-Maestre, C. Harden, R. Ewing, C. Carwford, H. Hill, Chemical standards in ion mobility spectrometry, Analyst 135 (2010) 1433–1442, https://doi.org/10.1039/B915202D.
[31] D. Meza-Morelos, R. Fernandez-Maestre, Caffeine and glucosamine mobility shifts by adduction with 2-butanol depended on the interaction energy, chare delocalization, and steric hindrance in ion mobility spectrometry, J. Mass Spectrom. 52 (2017) 823–829, https://doi.org/10.1002/jms.4026.
[32] M.T. Jafari, B. Rezaei, M. Javaheri, A new method based on electrospray ionization ion mobility spectrometry (ESI-IMS) for simultaneous determination of caffeine and theophylline, Food Chem. 126 (2011) 1964–1970, https://doi.org/10.1016/j.foodchem.2010.12.054.
[33] P. Dwivedi, B. Bendiak, B.H. Clowers, H.H. Hill, Rapid resolution of carbohydrate isomers by electrospray ionization ambient pressure ion mobility spectrometry-time-of-flight mass spectrometry (ESI-APIMS-TOFMS), J. Am. Soc. Mass Spectrom. 18 (2007) 1163–1175, https://doi.org/10.1016/j.jasms.2007.04.007.
[34] H. Holness, J. Almirall, Speciation effects of solvent chemistry on the analysis of drugs and explosives by electrospray ion mobility mass spectrometry, Int. J. Ion Mobil. Spectrom. 16 (3) (2013) 237–246, https://doi.org/10.1007/s12127-013-0136-2.

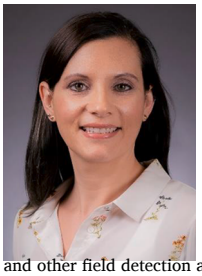

Lauryn E. DeGreeff earned her PhD in forensic chemistry from Florida International University in Miami, FL, where she is presently an associate professor in the Chemistry Department and the International Forensic Science Research Institute and where she carries out research in the area of volatiles analysis as it relates to vapor detection by canine and instruments. Prior to returning to FIU, Dr. DeGreeff conducted her research as part of the Chemistry Division at the US Naval Research Laboratory in Washington DC. She takes a chemistry-based approach to studying olfaction for the purpose of informing field vapor sampling practices. Her research focuses on trace vapor sampling, characterization, and generation in support of canine and other field detection approaches. Dr. DeGreeff regularly lectures on the dynamics of odor for the operational community and at national and international scientific conferences. She has also authored a many peer-reviewed manuscripts, holds four pending and completed patents, and is the editor of the book entitled *Canines: The Original Biosensor*, to be released in early 2022.